Received: 26 August 2020 | Revised: 8 December 2020 | Accepted: 14 December 2020

DOI: 10.1002/tbio.202000023

FULL ARTICLE

TRANSLATIONAL BIOPHOTONICS

Utilization of Raman spectroscopy to identify breast cancer from the water content in surgical samples containing blue dye

Thomas J. E. Hubbard[1,2,3,4] | **Alexander P. Dudgeon**[3] | **Douglas J. Ferguson**[1,2,4] | **Angela C. Shore**[1,2] | **Nicholas Stone**[1,2,3]

[1]Institute of Biomedical and Clinical Science, University of Exeter Medical School, Exeter, UK

[2]NIHR Exeter Clinical Research Facility, Royal Devon and Exeter Hospital, Exeter, UK

[3]Biomedical Physics Group, Department of Physics and Astronomy, University of Exeter, Exeter, UK

[4]Royal Devon and Exeter Hospital, Exeter, UK

Correspondence
Nicholas Stone, Institute of Biomedical and Clinical Science, University of Exeter Medical School, Exeter EX4 4QL, UK.
Email: n.stone@exeter.ac.uk

Funding information
Engineering and Physical Sciences Research Council, Grant/Award Number: EP/P012442/1; National Institute for Health Research, Grant/Award Number: II-LB-1117-20002

Abstract

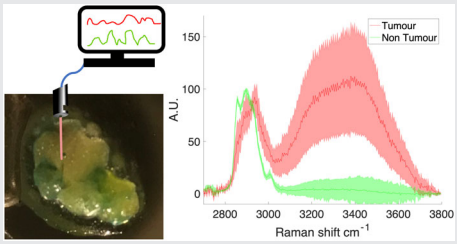

Breast conserving surgery (BCS) for breast cancer aims for optimal oncological results with minimal tissue excision. Positive margins due to insufficient resection results in significant numbers of patients requiring re-excision, which could be resolved with intra-operative margin analysis (IMA). High wavenumber (HWN) Raman Spectroscopy (RS) examines the difference in protein/lipid environment and water content in tissues. Fluorescence from haemoglobin and blue dye surgical pigments (commonly present in excised breast tissue) can confound HWN RS. We present a Raman system with 785 nm excitation laser and indium gallium arsenide camera capable of quantifying changes in water content in different environments (protein-rich and lipid-rich) by measuring the water/total area ratio (W/TAR) of the HWN spectrum. We demonstrate that haemoglobin and blue dye do not adversely affect water content analysis by the W/TAR calculation. Measurement of paired tumour/non-tumour human breast tissue specimens showed the biochemical differences between tissues, and spectral analysis with W/TAR demonstrated large differences in water content and that our Raman system can accurately differentiate between tumour and non-tumour tissue, even in the presence of surgical pigments. This provides proof of principle that this Raman system is suitable for further investigation with a view to providing IMA in the clinical environment.

KEYWORDS

breast cancer, breast neoplasms, mastectomy, Raman, Raman spectroscopy, segmental, spectrum analysis, surgical oncology

1 | INTRODUCTION

The aim of breast conserving surgery (BCS) in the treatment of breast cancer is to give optimal oncological result, with minimal excess tissue excision to maintain satisfactory cosmetic outcome. If there is residual tumour at the resected edge (positive margins) of the excised specimen, further resection is advised to reduce recurrence risk [1, 2]. This occurs in 17% of BCS in the UK [3], causing significant financial burden for the health service and patient anxiety [4]. There are currently no universally accepted methods of performing intra-operative margin analysis (IMA) in BCS.

Raman spectroscopy (RS) has shown excellent diagnostic capabilities in a number of cancers [5–7], with a sensitivity of 94% and specificity of 96% in diagnosing breast cancer [8]. A limitation is the time taken for spectral analysis with small sampling volumes which make it difficult to provide IMA in relevant time frames. The majority of Raman studies use the "fingerprint" spectral region of 800 to 1800 cm^{-1} due to its molecular specificity [7]; however, the high wavenumber (HWN) region of 2800 to 3800 cm^{-1} is capable of comparable diagnostic accuracy with simpler instrumentation [9], particularly when discriminating between significantly different pathological states [10–12]. The HWN region is sensitive to changes in protein, lipid and water, and the increased spectral intensity and less complex spectral analysis can reduce the time taken for signal acquisition [10].

The sensitivity of the HWN region to water is of interest, as tumours have a higher water concentration than surrounding normal tissue [13]. Garcia-Flores et al demonstrated with HWN RS that breast tumours in rat models had higher protein and water signals, and normal (adipose) tissue had a higher lipid and low water signals [14], which was confirmed in human breast tissue using HWN RS [15]. Barroso et al demonstrated the diagnostic ability of water content differences in oral squamous cell carcinoma with HWN RS [16]. A recent study used part of the HWN region to screen for areas of potential tumour in breast tissue [17]. These works suggest that HWN RS could be used for IMA in BCS but no studies to date have systematically explored this.

A clinical limitation of optical techniques is the presence of fluorescent surgical pigments [18]. Fluorescence occurs when the incident light excites fluorophores producing a strong broadband signal that overwhelms the weaker Raman signal, thus obliterating detection of Raman scattering. Two potentially fluorescent pigments are commonly found during BCS; haemoglobin (from human blood), and Patent Blue Dye ("BD") (injected into breast tissue for localization of sentinel lymph nodes). Lymph node localization using BD occurs in 23% to 54% of breast cancer operations [19]. In previous studies, samples with surgical pigments have either not been included [17], been washed [16] or the stained areas have been purposefully avoided [20] which limits their clinical application.

Our preliminary HWN RS experiments using a low wavelength (680 nm) excitation laser and CCD (a commonly used configuration [10, 16, 17]) demonstrated high background fluorescence, and complete obscuration of the Raman signal within the shot noise contribution from the considerable BD fluorescence. A laser with a longer, less energetic wavelength (785 nm) combined with an indium gallium arsenide (InGaAs) camera, more sensitive to the longer near infrared wavelengths, allows the HWN region to be measured with a reduced fluorescence background from biological tissue, while maintaining good signal-to-noise [21], which has been demonstrated in circumventing fluorescence in melanoma diagnosis [22].

The aim of this study was to identify an HWN Raman system able to differentiate between tumour and non-tumour human breast tissue specimens based on differences in water content and assess the diagnostic ability in the presence of surgical pigments, with a view to future IMA.

2 | METHODS

2.1 | Specimens for measurement

2.1.1 | Phantom construction

Gelatine phantoms were constructed by mixing porcine skin gelatine powder (Sigma Aldrich, Germany) with distilled water (total weight 10 g) to produce final concentrations of 85% to 95% water [23] (representative of protein-rich tissue with a high water content, to mimic tumour conditions).

BD gelatine phantoms were 90% water gelatine phantoms with Patent Blue V sodium salt (Sigma Aldrich) dissolved in the water at a 1% dye concentration (the concentration often injected into the breast). The dye was added at the mixing stage to the solution to produce a final phantom concentration of 0.01% or 0.1% BD, to mimic the concentration once the dye has diffused into the breast tissue and undergone handling. The solutions were stirred in a 55°C water bath until dissolved (20-30 minutes) then poured into 2.5 cm^3 moulds.

Soya bean oil phantoms were used as a lipid phantom (protocol adapted from Merritt et al[24]). Organic soya bean oil (Clearspring, UK) was mixed with a 4% lipid

volume of Triton X-100 (Sigma-Aldrich, Germany) for emulsification. The warmed solution was stirred for 5 minutes in a 55°C water bath before distilled water was added to produce a 10 mL total volume at the desired water concentration (range 40%-95% water, to mimic the physiologically normal range [25]). The solution was stirred for 5 minutes and underwent sonification with a Hielscher Ultrasonics UP100H Handheld ultrasonic processor (Hielscher Ultrasonics, Teltow, Germany) at 30 kHz with 100% amplitude and 100% pulse for 5×10 second pulses to create a liquid emulsion.

Phantoms were covered and stored at 5°C for 24 hours until Raman measurements were taken at room temperature.

2.1.2 | Pork meat phantoms

Pork chops with clearly demarked protein and lipid-rich sections (Tesco, UK) were used as a biological environment previously used to mimic human breast tissue [26]. Two pieces of pork meat (3 cm^3) were dissected. One was stained with 1% solution of Patent BD until it was visually as "blue" as excised breast tissue (judged by a surgeon). One was stained with a 7.5% solution of bovine haemoglobin (Sigma Aldrich) in distilled water: the estimated haemoglobin concentration in a breast specimen after excision and handling.

2.1.3 | Breast specimens

Human breast tissue samples were obtained from the Royal Devon and Exeter Hospital Tissue Bank as part of lumpectomy or mastectomy operations taken with informed consent during the patients' standard oncological treatment, having been approved by the local NIHR Exeter Clinical Research Facility (CRF) Tissue Bank, (CRF320; Tissue bank ethics number 16/SC/0162). Patients were females aged ≥18 years, able to consent, with a malignant tumour of ≥2 cm. The specimen was excised, sliced and a 2 to 5 mm^3 biopsy taken from the tumour, and a separate one from normal tissue, by a trained pathology practitioner. The research biopsies were snap-frozen in liquid nitrogen and stored at −80°C in the NIHR Exeter CRF Tissue Bank before being transferred to and frozen-sectioned at Gloucestershire Hospitals Pathology Department. An H&E section underwent routine histopathological analysis. The pathology classification and routine demographic data collected from patient notes were pseudonymously linked to the research specimens by the Tissue Bank. Bulk specimens were thawed at room temperature immediately prior to Raman measurements.

2.2 | Raman equipment configuration

Raman spectra were acquired for all experiments with a previously described fibre optic probe [27]. It is a standard stainless steel 23 gauge thin wall needle within which is a bundle of seven low-OH silica optical fibres stripped of their buffer (105 μm core, 0.22NA, Thorlabs) arranged as six collection fibres around one excitation fibre, giving an area of collection of 5.19×10^4 μm^2. Sampling volume modelled (not published) using phantoms was established to be of the order of 1 mm^3. Excitation light at a wavelength of 785 nm was provided by an IPS spectrum stabilized laser module (Innovative Photonic Solutions) through a 785 nm laser clean up filter (Thorlabs, NJ). Raman scattered light passed through an 830 nm long-pass edge filter (Semrock, Rochester) from the needle tip. The system provided a maximum power of 250 mW at 785 nm at the tip. The scattered light was passed through the same specification fibre to the entry port on a Kaiser Holospec Imaging Spectrograph (Kaiser Optical Systems Inc., Ann Arbour, Michigan) with a high throughput, broadband, transmissive holographic grating, HVG 800 (Kaiser) and coupled to an InGaAs line scan camera (iDus InGaAs 1.7 μm, Andor, Belfast, UK), thermoelectrically cooled to −70°C.

Spectra were calibrated daily using the spectral peaks of paracetamol, ethanol and acetylnitrile. A daily measurement with no laser or background light was taken for dark noise subtraction.

Measurements were obtained with the probe in light contact with the specimen and spectra were acquired for 5 seconds with five accumulations over the surface of the phantoms (n = 3 or 5) or breast specimen (n = 5-8). Measurements were obtained at random intervals over the largest surface of the specimen to ensure adequate representative sampling of tissue—the number of measurements taken depended on the surface area of the specimen and took less than 10 minutes to complete.

2.3 | Data processing analysis

Spectra were recorded using SOLIS software (Andor) and processed in MATLAB (MathWorks). The mean of the accumulations was taken, and a smoothed dark noise spectrum was subtracted (smoothing obtained by a Savitzky-Golay filter with a seventh order polynomial of the noise reading). The HWN region spectra underwent fluorescence baseline subtraction using a linear fit for the phantom spectra. A subtraction of a third order polynomial fit (previously used for HWN baseline subtraction in biological tissue [28, 29]) was applied to breast tissue spectra due to increased autofluorescence. For

visualization purposes only, spectra presented were normalized to the CH stretch of protein/lipid at 2940 cm^{-1}. The analysed spectra were not normalized. As a measure of water content, and to quantify changes within the HWN spectrum, the water/total area ratio was calculated, as described by Masson et al [29]. For each spectrum, the area under the curve (AUC) of the water peak (which also contains some contribution from the NH peak at 3280 cm^{-1}) between 3035 and 3680 cm^{-1}, and the AUC of the total HWN region between 2850 and 3680 cm^{-1} was calculated, then the AUC water peak was divided by AUC of the total HWN region to give the W/TAR. Spectra were analysed with this method, as it captures the entire water peak hence changes can be detected in both bound and unbound water [30], and the technique has been previously validated to detect water content changes in lipid rich and fluorescent tissues [29]. The mean W/TAR ratio and SD (SD) is used to describe each specimen. For scatter graphs, a linear fit was calculated based on all points with quality of fit described by the root mean square error.

Statistical analysis to compare W/TAR between specimens was performed by two-sided student *t* test or one-way analysis of variance (ANOVA) depending on number of groups and statistical significance $P < .05$.

3 | RESULTS

3.1 | Quantification of change in water content

Figure 1 presents the results in two different environments, Figure 1A shows a protein/water environment (gelatine phantoms) and Figure 1B shows a lipid/water environment (soya bean oil phantom).

In both environments, there is a change in the HWN spectra with a change in the water content. There was a relative decrease in the OH stretch region (3035-3680 cm^{-1}) when normalized to the CH stretch region (2850-3035 cm^{-1}) (as measured by a decrease in W/TAR), with a decrease in water

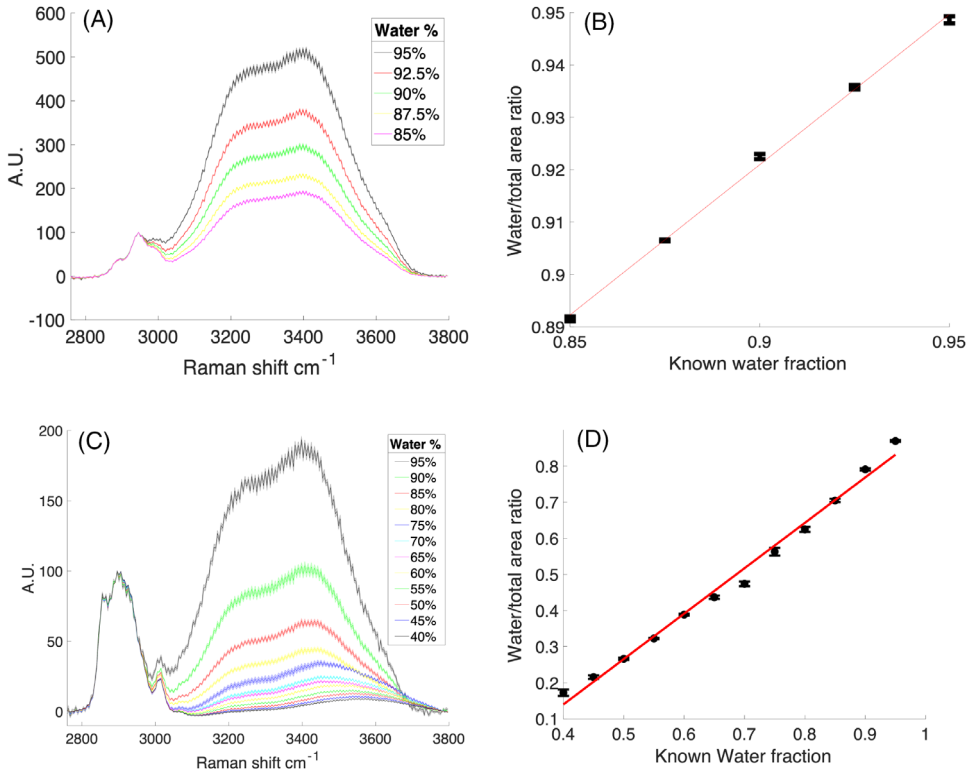

FIGURE 1 Demonstrating the ability of the Raman system to measure and quantify changes in water concentration in two different environments: A, Mean Raman spectra normalized to peak at 2940 cm^{-1} of each gelatine phantom with shading either side in the same colour ±1 SD. B, Mean water/total area ratio (W/TAR) of each gelatine phantom (not normalized), error bars ±1 SD Red line is line of best fit (gradient = 0.57, root mean square error [RMSE] 0.0009). C, Mean Raman spectra normalized to peak at 2940 cm^{-1} of each soya bean oil phantom with shading either side in the same colour ±1 SD. D, Mean W/TAR (not normalized) of each soya bean oil phantom, error bars ±1 SD (gradient = 1.26, RMSE = 0.02). In all graphs, mean represents a mean of n = 5 measurements taken from different points of each specimen

content. There was a linear relationship between W/TAR and known water content in the phantoms—the gradient for gelatine phantom W/TAR was 0.57, and the gradient for soya bean oil phantom W/TAR was 1.26.

3.2 | Overcoming fluorescence of surgical pigments

Figure 2 demonstrates that, in the presence of haemoglobin and BD pigment, HWN Raman signal was unaffected with no significant difference in the mean W/TAR between specimens (untreated pork 0.82 [SD 0.08]; haemoglobin treated pork 0.81 [SD 0.06]; BD treated pork 0.85 [SD 0.02]; $P = .49$ one-way ANOVA).

Due to particular concerns for BD fluorescence, measurements were performed in BD spiked gelatine phantoms that had concentrations expected in excised breast tissue. There was a slight trend towards increased mean W/TAR in the presence of BD (no BD W/TAR = 0.92 [SD 0.007], 0.01% BD W/TAR = 0.93, [SD 0.008], 0.1% BD W/TAR = 0.93, [SD 0.003]), but this was not significantly different ($P = .28$; one-way ANOVA). The maximum range of change in individual W/TAR was 3% (range 0.91-0.94) which, based on the gradient of gelatine phantoms in Figure 1, is equivalent to only a 5% difference in water content.

3.3 | Differentiating between tumour and non-tumour human breast tissue

Paired samples from nine patients (tumour samples n = 9, non-tumour samples n = 9) were measured. All patients were female, mean age 65 (range 41-84), three were pre-menopausal and six post-menopausal. Five underwent a lumpectomy and four mastectomy for invasive breast carcinoma with a mean tumour size of 30 mm (range 19-51 mm). Six had invasive ductal carcinoma, two lobular carcinoma and one mixed carcinoma. All tumours were oestrogen receptor positive, with one also

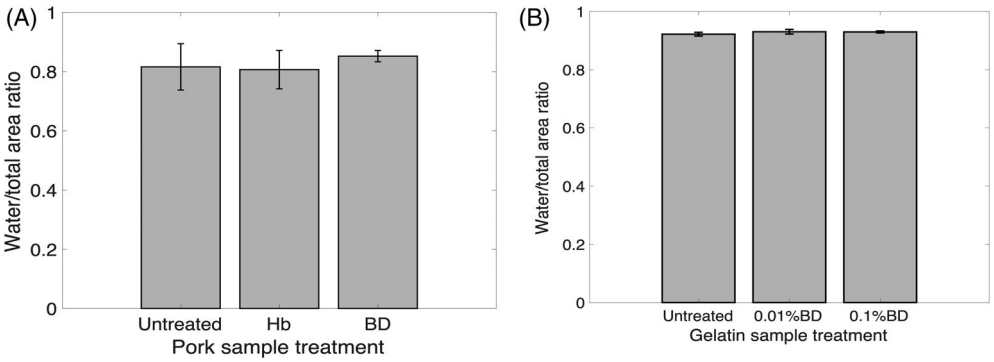

FIGURE 2 Graphs showing the effect of surgical pigments on the mean water/total area ratio (W/TAR) for High wavenumber (HWN) Raman spectra. A, Bar chart showing mean W/TAR in different treatments of pork specimens; untreated—no pigment, Hb—pork treated with haemoglobin pigment, BD—pork treated with patent blue dye pigment. B, Bar chart showing mean W/TAR in different concentrations of Blue Dye (BD) in 90% water gelatine phantoms. Data are not normalized; Error bars ±1 SD

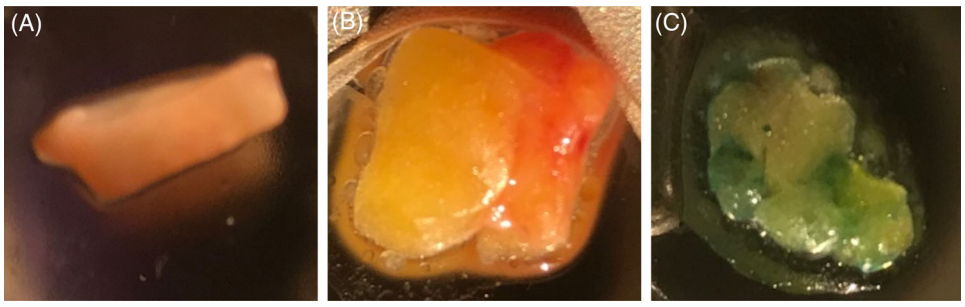

FIGURE 3 Photos of breast tissue included in the study, with different pigments. A, Breast biopsy tissue with minimal additional pigments (though a small amount of haemoglobin still present). B, Breast biopsy tissue obviously stained with haemoglobin pigment. C, Breast biopsy tissue stained with BD

HER2 positive and eight had associated ductal carcinoma in situ. Eight had a sentinel lymph node biopsy, and one an axillary node clearance, with four having axillary lymph node metastatic deposits.

All specimens had some natural haemoglobin pigment visible, and in four BD was seen (Figure 3).

All specimens (n = 18) were measured to obtain a total of 116 spectra. The mean spectrum from all tumour specimens (n = 9) and all non-tumour specimens (n = 9) show clear spectral difference between the specimen types (Figure 4A). Tumour specimens have a narrow peak at 2900 to 2950 cm^{-1} from the CH_2 asymmetric stretch, and a peak in the OH stretch region between 3050 and 3680 cm^{-1} [31] suggesting tumour tissue has a high protein content and high water content. Non-tumour specimens have a broader peak at 2855 to 2950 cm^{-1} CH_3 stretch region, consistent with lipid [31], and minimal signal in the OH stretch region—suggesting predominantly fatty tissue with a low water content.

The W/TAR was calculated for each spectrum, and the mean W/TAR of spectra from tumour tissue specimens (mean W/TAR = 0.7559; SD 0.1022) was significantly higher than non-tumour tissue (mean W/TAR = 0.1587; SD 0.1339) ($P = 7 \times 10^{-6}$; t test) (Figure 4B). Using a W/TAR cut off of 0.5 for diagnosis, for example, samples with W/TAR <0.5 were classified as non-tumour, and samples with W/TAR ≥0.5 were classified as tumour, all samples were correctly classified, suggesting W/TAR analysis can accurately differentiate between tumour and non-tumour tissue.

To assess the diagnostic performance in the presence of BD, samples were grouped and W/TAR was analysed according to tumour or non-tumour classification, and whether there was BD present (with BD) or not (no BD) (Figure 5). One-way ANOVA of all groups was significantly different ($P = .00005$); multi-technique comparison showed that tumour, with BD (n = 4; mean W/TAR = 0.7415; SD 0.0795) was similar to tumour, no BD (n = 5; mean W/TAR = 0.7675; SD 0.1255) ($P = .5048$); and non-tumour, with BD (n = 4; mean W/TAR 0.0957; SD 0.0639) was similar to non-tumour, no BD (n = 5; mean W/TAR 0.2091; SD 0.1602) ($P = .987$). Comparison between the mean W/TAR tumour (both BD and no BD) compared to non-tumour, both BD and no BD, showed statistical significance ($P < .001$). The presence of BD did not significantly alter the Raman signal between the same tissue types, and W/TAR can differentiate between tumour and non-tumour tissue in the presence of BD.

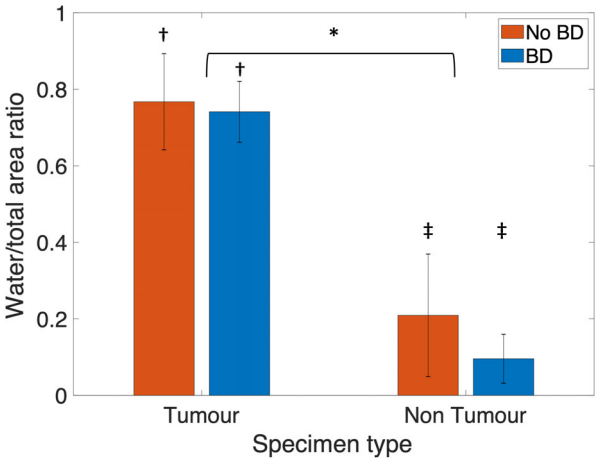

FIGURE 5 Bar chart showing the mean water/total area ratio (W/TAR) for human breast tissue specimens according to specimen type, and whether there was blue dye present (BD) or not (no BD). Data not normalized. † denotes comparison between tumour specimens W/TAR, $P > .05$, and ‡ denotes comparison between non-tumour specimens W/TAR, $P > .05$. When W/TAR of either group of † was compared to either group of ‡, it reached statistical significance $P < .001$; denoted by *

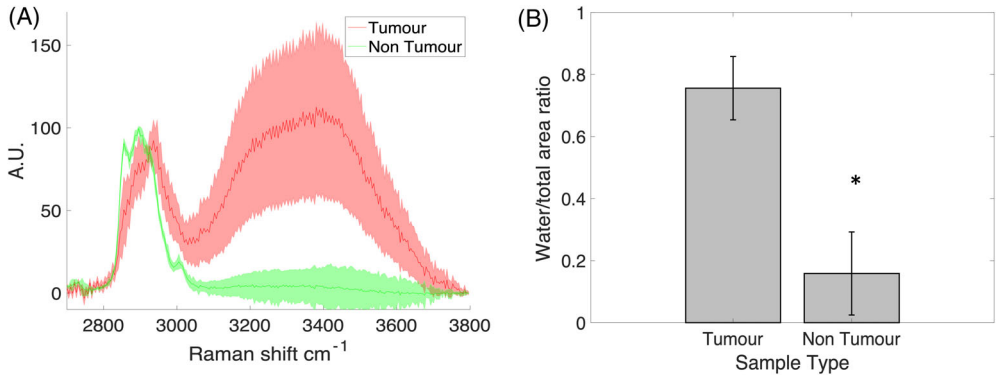

FIGURE 4 High wavenumber (HWN) Raman differentiating between tumour and non-tumour human breast tissue. A, Raman spectrum of tumour (n = 9) (red) and non-tumour (n = 9) (green) human breast tissue, normalized to peak at 2940 cm^{-1}. Central spectrum is mean spectrum with outlying lines and shading either side in the same colour ±1 SD. B, Bar Graph of mean water/total area ratio (W/TAR) according to sample type; data not normalized; error bars ±1 SD * denotes significant difference in comparison of the means; $P = 7 \times 10^{-6}$; t test

4 | DISCUSSION

This study demonstrates a Raman system that can quantify changes in water content in different micro-environments (protein-rich and lipid-rich) and can perform accurate HWN RS tissue diagnosis in the presence of haemoglobin and BD. We have demonstrated a method of spectral analysis (W/TAR) that can assess the difference in water content of human breast specimens and demonstrates a significant difference between tumour and non-tumour tissue; using a cut-off of 0.5, the W/TAR can accurately differentiate between tumour and non-tumour breast tissue.

The HWN spectra in protein-rich and lipid-rich micro-environments demonstrates that water content changes can be detected by HWN RS, and quantified by calculation of the W/TAR. The relationship between W/TAR and specimen water content is dependent on the waters' microenvironment: in a 90% water protein-rich phantom the W/TAR was 0.92, whereas in a 90% water lipid-rich phantom the W/TAR was 0.82. The rate of change of W/TAR is also dependent on water microenvironment—exemplified by the different linear fit gradients. This demonstrates that quantification of water content using HWN RS is dependent on the microenvironment of the water. Biological tissues have areas of different protein and lipid ratios so quantification of changes in water content requires detailed scrutiny of the CH region and quantification of protein-to-lipid ratio. Therefore, absolute W/TAR cannot be used as a standard measure of water quantification across tissue types, but these results show that it can demonstrate differences in water concentration in the different environments found in breast tissues.

Previous work demonstrating the differences in the HWN spectra of tumour and non-tumour breast tissue, have been limited to rat models [14], the laboratory environment [15] or have not captured the water peak [17]. This study demonstrates, with clinical specimens, that breast tumours are protein and water rich environments, and non-tumour breast tissues are lipid-rich, with a low water content and the simple analysis of W/TAR can analyse tissue based on water content. By using a laser with a longer wavelength combined with an InGaAs camera, we have avoided inducing fluorescence from surgical pigments and demonstrated that the diagnostic ability was unaffected by the presence of BD.

There are some limitations to this study. Frozen samples may have a different "true" water content compared to fresh tissue. However, the samples were immediately snap-frozen on collection and measured rapidly on thawing, reducing dehydration time which minimizes differences in water content from fresh samples. Biopsy samples were small compared to larger breast specimens measured in IMA; however, one would expect more rapid dehydration from smaller samples (with increased surface area), and so the differences observed between tissue types may be an underestimate. The probe sampling volume is not suitable for analysing a large specimen in a timely manner for IMA. However, now the proof of principle to obtain diagnostic HWN Raman signals has been achieved the probe can be optimized to analyse the larger tissue volumes needed for IMA. Other work in the group has demonstrated the ability of deep Raman techniques to probe buried regions of high water content within large volumes of biological tissues [26]. This study was performed in a small number of samples; however, they have paired control samples allowing for robust analysis of the diagnostic ability of W/TAR to differentiate between tissue types in an individual. These findings should be validated in future studies, by testing the cut-off threshold on a larger data set of freshly excised samples (non-frozen).

5 | CONCLUSIONS

We present an HWN Raman system capable of signal acquisition in the presence of the surgical pigments of haemoglobin and patent BD, and quantifying changes in water content. We demonstrate in human breast tissue, for the first time, the ability to differentiate between tumour and non-tumour tissue based on water content in the presence of surgical pigments of haemoglobin and patent BD with HWN RS. This approach warrants further investigation with a view to providing future IMA in the clinical environment.

ACKNOWLEDGMENTS

A. C. S. was supported by the NIHR Exeter Clinical Research Facility. The study was supported by the NIHR Exeter Clinical Research Facility Tissue Bank Team. The views expressed in this manuscript are the views of the authors and not those of the NIHR or the Department of Health and Social Care. A. D. was supported by NIHR I4i grant ref number II-LB-1117-20002 - DOLPHIN-VIVO - Diagnosis Of LymPHoma IN VIVO. N. S. was supported by EPSRC grant ref number EP/P012442/1.

CONFLICT OF INTEREST

The authors declare no conflict of interest.

DATA AVAILABILITY STATEMENT

The data that support the findings of this study are available from the corresponding author upon reasonable request.

ETHICS STATEMENT

This study was approved by the NIHR Exeter Clinical Research Facility Tissue Bank, (Tissue bank ethics number 16/SC/0162).

PATIENT CONSENT STATEMENT

All participants provided written informed consent prior to enrolment in the study.

ORCID

Thomas J. E. Hubbard https://orcid.org/0000-0003-4593-0853

REFERENCES

[1] *National Institute for Health and Care Excellence (NICE) in Early and Locally Advanced Breast Cancer: Diagnosis and Management*, London, NICE, **2018**.
[2] N. Houssami, P. Macaskill, M. Luke Marinovich, M. Morrow, *Ann. Surg. Oncol.* **2014**, *21*, 717.
[3] S. S. Tang, S. Kaptanis, J. B. Haddow, G. Mondani, B. Elsberger, M. K. Tasoulis, C. Obondo, N. Johns, W. Ismail, A. Syed, P. Kissias, M. Venn, S. Sundaramoorthy, G. Irwin, A. S. Sami, D. Elfadl, A. Baggaley, D. D. Remoundos, F. Langlands, P. Charalampoudis, Z. Barber, W. L. S. Hamilton-Burke, A. Khan, C. Sirianni, L. A. G. Merker, S. Saha, R. A. Lane, S. Chopra, S. Dupre, A. T. Manning, E. R. St John, A. Musbahi, N. Dlamini, C. L. McArdle, C. Wright, J. O. Murphy, R. Aggarwal, M. Dordea, K. Bosch, D. Egbeare, H. Osman, S. Tayeh, F. Razi, J. Iqbal, S. F. C. Ledwidge, V. Albert, Y. Masannat, *Eur. J. Cancer.* **2017**, *84*, 315.
[4] Y. Grant, R. Al-Khudairi, E. St John, M. Barschkett, D. Cunningham, R. Al-Mufti, K. Hogben, P. Thiruchelvam, D. Hadjiminas, D. Leff, *Br. J. Surg.* **2019**, *106*, 384.
[5] T. J. E. Hubbard, A. Shore, N. Stone, *Analyst* **2019**, *144*, 6479.
[6] G. Shetty, C. Kendall, N. Shepherd, N. Stone, H. Barr, *Br. J. Cancer.* **2006**, *94*, 1460.
[7] H. J. Butler, L. Ashton, B. Bird, G. Cinque, K. Curtis, J. Dorney, K. Esmonde-White, N. J. Fullwood, B. Gardner, P. L. Martin-Hirsch, M. J. Walsh, M. R. McAinsh, N. Stone, F. L. Martin, *Nat. Protoc.* **2016**, *11*, 664.
[8] A. S. Haka, K. E. Shafer-Peltier, M. Fitzmaurice, J. Crowe, R. R. Dasari, M. S. Feld, *Proc. Natl. Acad. Sci. U. S. A.* **2005**, *102*, 12371.
[9] S. Koljenovic, T. C. B. Schut, R. Wolthuis, B. de Jong, L. Santos, P. J. Caspers, J. M. Kros, G. J. Puppels, *J. Biomed. Opt.* **2005**, *10*, 031116.
[10] K. Aubertin, J. Desroches, M. Jermyn, V. Q. Trinh, F. Saad, D. Trudel, F. Leblond, *Biomed. Opt. Express.* **2018**, *9*, 4294.
[11] K. M. Curtis, University of Exeter **2017**.
[12] A. Nijssen, K. Maquelin, L. F. Santos, P. J. Caspers, T. C. B. Schut, J. C. den Hollander, M. H. Neumann, G. J. Puppels, *J. Biomed. Opt.* **2007**, *12*, 034004.
[13] R. Damadian, *Science* **1971**, *171*, 1151.
[14] A. García-Flores, L. Raniero, R. Canevari, K. J. Jalkanen, R. Bitar, H. Martinho, A. Martin, *Theor. Chem. Acc.* **2011**, *130*, 1231.
[15] H. Abramczyk, B. Brozek-Pluska, J. Surmacki, J. Jablonska-Gajewicz, R. Kordek, *J. Biophys. Chem.* **2011**, *2*, 159.
[16] E. Barroso, R. Smits, T. Bakker Schut, I. Ten Hove, J. Hardillo, E. Wolvius, R. Baatenburg de Jong, S. Koljenovic, G. Puppels, *Anal. Chem.* **2015**, *87*, 2419.
[17] Z. Liao, M. G. Lizio, C. Corden, H. Khout, E. Rakha, I. Notingher, *J. Raman Spectrosc.* **2020**, *51*, 1986.
[18] T. M. Bydlon, W. T. Barry, S. A. Kennedy, J. Q. Brown, J. E. Gallagher, L. G. Wilke, J. Geradts, N. Ramanujam, *PLoS One* **2012**, *7*, e51418.
[19] K. O. Lawrence G, C. Lagord, S. Cheung, J. Sidhu, C. Sagar, *Second all Breast Cancer Report*, London, National Cancer Intelligence Network, **2011**, p. 42.
[20] D. W. Shipp, E. A. Rakha, A. A. Koloydenko, R. D. Macmillan, I. O. Ellis, I. Notingher, *Breast Cancer Res.* **2018**, *20*, 69.
[21] I. P. Santos, P. J. Caspers, T. Bakker Schut, R. van Doorn, S. Koljenović, G. J. Puppels, *J. Raman Spectrosc.* **2015**, *46*, 652.
[22] I. S. P. Santos, P. J. Caspers, T. C. B. Schut, R. van Doorn, V. N. Hegt, S. Koljenović, G. J. Puppels, *Anal. Chem.* **2016**, *88*, 7683.
[23] S. Kalyanam, R. D. Yapp, M. F. Insana, *J. Biomech. Eng.* **2009**, *131*, 081005.
[24] S. Merritt, G. Gulsen, G. Chiou, Y. Chu, C. Deng, A. E. Cerussi, A. J. Durkin, B. J. Tromberg, O. Nalcioglu, *Technol. Cancer Res. Treat.* **2003**, *2*, 563.
[25] S. Srinivasan, B. W. Pogue, S. Jiang, H. Dehghani, C. Kogel, S. Soho, J. J. Gibson, T. D. Tosteson, S. P. Poplack, K. D. Paulsen, *Proc. Natl. Acad. Sci. U. S. A.* **2003**, *100*, 12349.
[26] A. Ghita, T. Hubbard, P. Matousek, N. Stone, *Anal. Chem.* **2020**, *92*, 9449.
[27] I. E. I. Petterson, J. C. Day, L. M. Fullwood, B. Gardner, N. Stone, *Anal. Bioanal. Chem.* **2015**, *407*, 8311.
[28] E. Barroso, T. Bakker Schut, P. Caspers, I. P. Santos, E. Wolvius, S. Koljenović, G. Puppels, *J. Raman Spectrosc.* **2018**, *49*, 699.
[29] L. E. Masson, C. M. O'Brien, I. J. Pence, J. L. Herington, J. Reese, T. G. van Leeuwen, A. Mahadevan-Jansen, *Analyst* **2018**, *143*, 6049.
[30] M. Unal, S. Yang, O. Akkus, *Bone* **2014**, *67*, 228.
[31] Z. Movasaghi, S. Rehman, I. U. Rehman, *Appl. Spectrosc. Rev.* **2007**, *42*, 493.

How to cite this article: Hubbard TJE, Dudgeon AP, Ferguson DJ, Shore AC, Stone N. Utilization of Raman spectroscopy to identify breast cancer from the water content in surgical samples containing blue dye. *Translational Biophotonics*. 2021;e202000023. https://doi.org/10.1002/tbio.202000023